Energetic evaluation of a power plant integrated with a piperazine-based CO_2 capture process

Hanne M. Kvamsdal [a,*], Matteo C. Romano [b], Leen van der Ham [c], Davide Bonalumi [b], Peter van Os [c], Earl Goetheer [c]

[a] *SINTEF Materials and Chemistry, Department of CO_2 Capture Process Technology, Post Box 4760 Sluppen, N-7465 Trondheim, Norway*
[b] *Politecnico di Milano – Department of Energy, Via Lambruschini, 4, 20156 Milano, Italy*
[c] *TNO, Netherlands Organisation for Applied Scientific Research, Department of Gas Treatment, Leeghwaterstraat 46, 2628 CA Delft, The Netherlands*

1. Introduction

According to a recent study made by Global Carbon Project, a group of international scientists from the UK, Norway and Germany, global greenhouse gas emissions from burning fossil fuels reached the highest levels in human history in 2012 and are likely to grow even further in the near future (EnergyMarketPrice, 2013). Most of these increased emissions are caused by the increasing use of coal (43%), oil (33%), and natural gas (18%). Though there has recently been increased focus on exploring renewable energy sources, this has not been enough to achieve a decrease in the emission of CO_2. A number of studies have concluded that Carbon Capture and Storage (CCS) should play a major role to meet the international objective (United Nations Framework Convention on Climate Change, 2010) of limiting the global average temperature increase to not more than $2\,°C$ above preindustrial levels. Though CCS has been advocated for 15–20 years, there are still no large scale facilities for the whole CCS chain. In addition to the uncertainty related to storage, the main technological issue delaying implementation of CCS is the high cost of capture. There is, therefore, a clear need to keep on developing more efficient and less cost-intensive capture technologies.

Though post-combustion technologies can be employed for CO_2 capture from any industrial source, this work focuses on post-combustion capture from the flue gas of coal-fired power plants. The most appropriate separation technology in power plants is still considered to be chemical absorption. The most conventional and simple process for chemical absorption involves counter-current absorption of CO_2 in an alkanolamine at a relatively low temperature ($30–50\,°C$) and regeneration of the solvent at a higher temperature ($>100\,°C$) and a pressure of approximately 2 bar. However, the state of the art system based on mono-ethanolamine (MEA) is costly. As a result, severe research efforts have been applied during the last 15 years focussing on three main development areas: capture plant configurations, integration between the capture plant and power plant, and solvent systems.

Cousins et al. (2011) have made a survey of several process flow sheet modifications proposed in this period based on a literature and patent review. The reviewed processes are classified

according to their modifications to the conventional process: (1) inter-cooling of the absorber to reduce the effect of the temperature bulge, (2) heat integration of the stripper to reduce the exergy losses along the column, (3) split flow regimes to obtain a more optimal temperature profile in the absorber, (4) vapour recompression to replace some of the steam required in the reboiler for the stripping process, and (5) matrix stripping, which is an advanced multicolumn, multi pressure stripping process proposed by Rochelle and Oyenekan (2008) and Oyenekan and Rochelle (2006). In the analysis by Cousins et al. (2011) these proposed process modifications are mostly based on MEA as solvent system and the performance results are mainly obtained by flowsheet simulations. All the modifications seem to exhibit improved energy performance, but they all imply added process units and process complexity. Thus it remains to see if the improved energetic performance can counteract the negative effect of possible increased capital cost and possibly more advanced control system. Except maybe for Lean Vapour Compression (LVC), which has been demonstrated by Knudsen et al. (2011) at the pilot plant in Esbjerg, none of the proposed modifications mentioned by Cousins et al. have been studied in more detail experimentally on pilot-scale.

Studies on the interaction between the power plant and capture plant have mostly been focussed on improvements of the energy performance, by optimizing the thermal integration (Pfaff et al., 2010; De Miguel Mercader et al., 2012; Giuffrida et al., 2013). Recently, operational flexibility has also gained interest (IEAGHG, 2012; NETL, 2012; Jordal et al., 2012; Roeder et al., 2013). Part load operations, flexibility and rapid start-up and shut-down have become increasingly important with power market liberalization and the increasing share of non-predictable renewable energy sources like wind and solar power. In most of the developed countries, flexibility is today a primary need for the market of combined cycles, which are required to contribute to grid stability and to gain the benefits of variable energy prices between peak and off-peak hours. However, flexible operation is becoming increasingly important, at least for the mid merit market, also for steam cycle-based pulverized coal power plants, which used to be typically designed and are usually operated for base load demand. Therefore, when assessing a power plant including a CO_2 capture section, additional operating variables, also affecting the design of important components, have to be optimized to improve the flexibility of the plant, the performance at off-design operations and ultimately maximize the profitability of the plant over its lifetime.

Several alternatives to the conventional solvent system using aqueous MEA are being developed. A promising option is the solvent system based on concentrated piperazine (PZ), which has been extensively studied by Gary Rochelle and his research group at the University of Texas, Austin. An important advantage of PZ with respect to other solvents is its high thermal stability; operating temperatures up to 150 °C can be used without any severe thermal degradation. For MEA, the corresponding maximum temperature is 120 °C. A possible disadvantage of PZ is its ability to form solids. However, it has been concluded that 8 M PZ (8 mol/kg water, 40 wt%) concentration can be used at a loading between 0.26 and 0.42 mol CO_2/equivalent PZ ($nCO_2/2nPZ$) without risk of solids precipitation down to 20 °C (Rochelle et al., 2011). Furthermore, PZ has acceptable volatility, but slightly higher than MEA. However, the rate of CO_2 absorption is substantially enhanced compared to MEA. PZ is also much less susceptible to oxidative degradation (Voice and Rochelle, 2011). Since the temperature bulge in the absorber is inappropriately high with this solvent system, inclusion of inter-cooling of the absorber has a very positive effect. Furthermore, since the stripping process can be operated at higher temperature than for MEA, the stripper column can be replaced with flash tanks that are operated at a higher pressure and temperature. Configurations using two flash tanks in series operating at different

Table 1
Composition and heating values of the South African Douglas Premium coal used in this study.

C	66.52
N	1.56
H	3.78
O	5.46
S	0.52
Ash	14.15
Moisture	8.01
Lower heating value (LHV), MJ/kg	25.170
Higher heating value (HHV), MJ/kg	26.230
CO_2 emission factor, g/kWh$_{LHV}$	348.6

pressures have shown very promising energy performance results compared to the conventional MEA-based process (Van Wagener and Rochelle, 2011; Frailie et al., 2013). Their results are based both on pilot plant experiments as well as on process flowsheet simulations using Aspen Plus®. Quite recently, the use of a single flash tank has been proposed (Lin et al., 2013). Though some economic numbers were recently presented at the TCCS-7 conference (Frailie et al., 2013), a more extensive techno-economic evaluation is still required. The integration between a PZ-based capture plant with the upstream power-plant has so far only been the subject of an exploratory study (Van der Ham et al., 2013), which confirmed the promising energetic performance of such a system.

The main purpose of the present paper is to perform a detailed study and optimization of the energetic performance of a PZ-based CO_2 capture plant integrated with a coal-fired power plant. This performance will be compared both to a power plant without CO_2 capture and to a power plant integrated with an MEA-based capture plant. Greenfield installations have been considered for the capture plants and issues related to adaptability of the existing power plant components for retrofitting are not investigated. The main issues that influence the flexibility of the PZ-based plants assessed in this work are additionally discussed on a qualitative basis.

2. Basis for the study

2.1. Power plant description

The power plant is defined according to EBTF (2011) guidelines and is based on an ultra-supercritical pulverized coal boiler, generating superheated and reheated steam at 270/60 bar and 600/620 °C steam conditions. The plant is fed with 1657 MW$_{LHV}$ of low sulphur South African bituminous Douglas Premium, with composition and heating values reported in Table 1.

The schematic of the reference power plant without CO_2 capture is shown in Fig. 1. Primary and secondary air is heated up in a trisector Ljungstrom air preheater (APH). Primary air (25% of the total combustion air) provides means of coal drying and is used for the transport of the pulverized coal from the mills to the burners. Secondary air is injected at different levels in the boiler according to an air-staging system for primary control of NO_x emissions. An oxygen content of 2.9% in the flue gas is maintained by a proper air excess. Heat losses of 0.35% of the LHV heat input and of 0.5% of the heat transferred in the heat exchanger banks have been considered for incomplete combustion and radiation losses.

Exhaust gases leave the boiler after the economizer banks at the temperature of 350 °C and are sent to a selective catalytic reduction (SCR) unit for NO_x abatement. Flue gases are then cooled down to 120 °C in the air preheater, and de-pulverized with fabric filters. Air in-leakages have been assumed in the boiler and in the fabric filters, respectively equal to 1% and 5% of the total flue gas mass flow rate. These fresh air infiltrations are due to the negative pressure kept in the boiler by a proper balance of the forced and induced draft fans. De-pulverized flue gas is sent to the wet flue gas desulfurizer
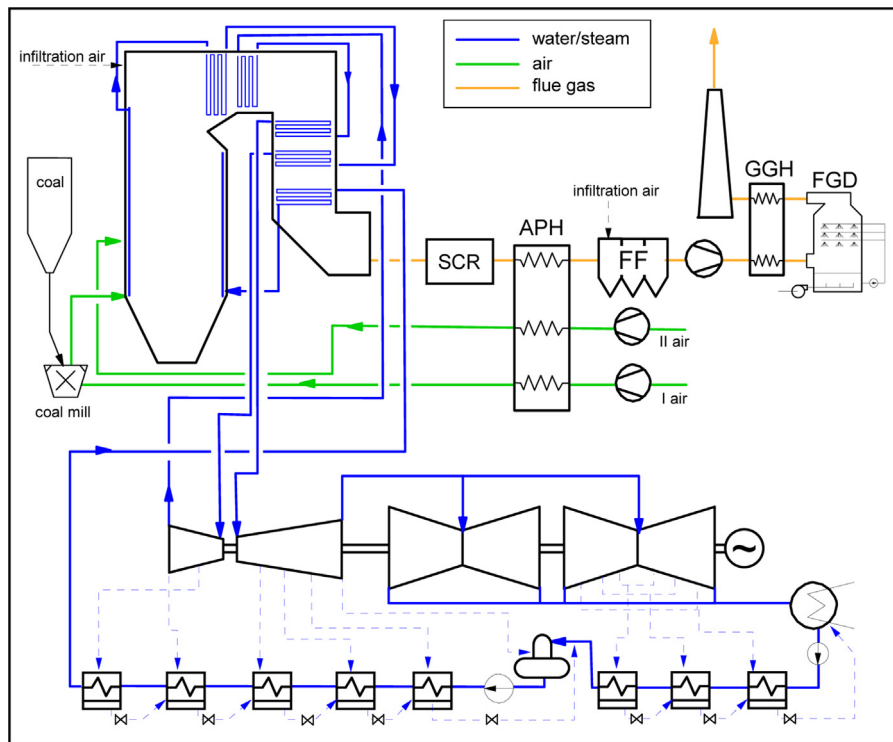
Fig. 1. Schematic of the reference power plant without CO_2 capture.

(FGD) for SO_2 removal. A regenerative gas–gas heater (GGH) is used to heat up the saturated gas from the FGD absorber to secure the necessary lift of the flue gas and reduce the visibility of the plume at the stack. Electric consumptions of boiler auxiliaries (fuel handling and milling, ash removal and handling, FGD) are mainly derived from data reported in NETL (2002, 2003).

A condensing pressure of 0.048 bar (32.1 °C) has been assumed. Heat from the condenser (and from the other plant units in the capture cases) is rejected to the environment by means of cooling towers. Auxiliaries for heat rejection have not been calculated in details, but overall consumptions of 0.008 kJ$_e$ per kJ of thermal power dissipated have been assumed. Before feeding the boiler, condensate is preheated in four low-pressure (including the deaerator) and five high-pressure regenerative preheaters.

The steam turbine has a four-flow LP section. A crossover pressure of 5.2 bar has been assumed for the benchmark case without capture, according to EBTF (2011). However, as explained further on, in capture cases steam for solvent regeneration is assumed to be extracted from the crossover and hence its pressure has been adapted in order to match the solvent regeneration temperature. The steam turbine is calculated with a stage-by-stage model (Lozza, 1990), where stage efficiency is calculated as a function of its non-dimensional parameters and of the moisture fraction when present in the low pressure stages. The high pressure turbine section features high reaction degree-high efficiency stages. The low pressure turbine section is based on two double-flow cylinders. The geometry of the last turbine stage is fixed and assumed compatible with large state-of-the-art steam turbines (Leyzerovich, 2007). In particular, a last blade height of 1.04 m and a mean diameter of 3.2 m, leading to an exhaust area per flow of 10.4 m^2, have been assumed. This size leads to a steam discharge axial velocity of 220 m/s from the last stage, with the given plant thermal input. In the reference plant without CO_2 capture, the resulting overall isentropic efficiencies of the turbine cylinders are 93.2%, 94.6% and 88.2% (including leaving losses) for HP, IP and LP sections respectively.

The mass and energy balances of the power plant are calculated with the in-house GS code (Gecos, 2013). The main assumptions used for the calculations are resumed in Table 2. Most of them are derived from the European benchmarking task force document (EBTF, 2011).

2.2. Capture plant description

The process configuration of the capture plant is based on the most recent publication by Frailie et al. (2013). Compared to the original process described by Rochelle et al. (2011), the most important change to the basic two-stage flash desorption configuration involves the addition of a cold rich by-pass, which improves the process energy performance. The used capture process flowsheet is shown in Fig. 2.

Before the CO_2-containing flue gas is fed to the absorption part of the capture plant, it first enters a direct contact cooler where the water content of the flue gas is reduced. This part is not shown in Fig. 2. Next, a blower is used to feed the flue gas to the bottom of the intercooled absorption column, where CO_2 is being absorbed by the counter-currently flowing aqueous PZ solution. A pump is used to increase the pressure of the rich solvent to about 10–20 bar, after which the solvent is heated against the regenerated lean solution in two subsequent heat exchangers. In between the two heat exchangers, a portion of the rich solution is split off from the main stream and used as 'cold' feed to the two flashes, meaning it is by-passing the second heat exchanger. After heating, the rich solution enters a series of two flash tanks, where the absorbed CO_2 is desorbed and leaves as a vapour. These flash tanks are heated to a temperature of 150 °C; up to this temperature PZ is still hardly affected by degradation (Freeman et al., 2010b). Both flashes are equipped with small packed sections at the top, above which the cold rich by-pass stream is fed. In this way, the outgoing gas streams are being pre-cooled and some thermal energy can be recovered within the flash tanks.
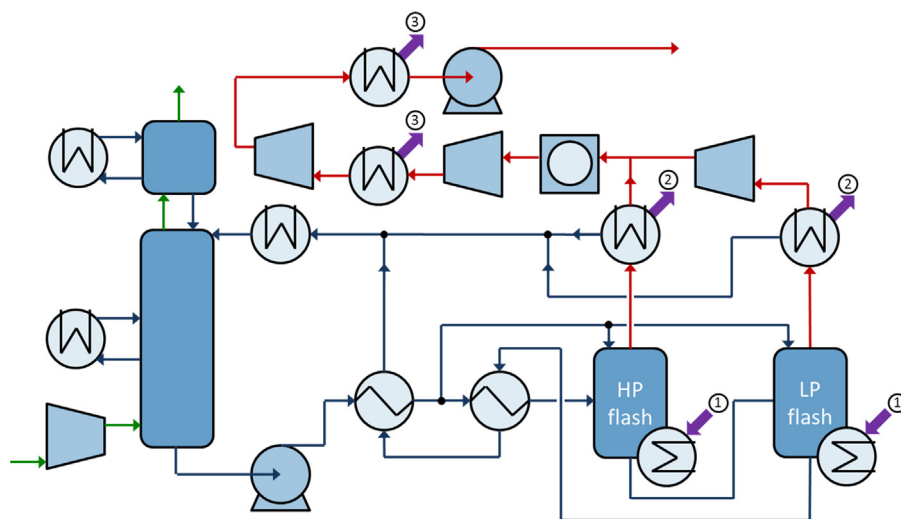
Fig. 2. Flowsheet of a CO_2 capture plant with a two-stage flash and cold rich by-pass, based on the flow-sheet presented by Frailie et al. (2013). Bold purple arrows are used to indicate the locations that are integrated with the power plant. (For interpretation of the references to color in this text, the reader is referred to the web version of the article.)

The regenerated solution is first cooled against the rich solution in the two previously-mentioned heat exchangers, and subsequently cooled to a temperature of 40 °C in an additional cooler. Desorbed CO_2 is compressed up to a final pressure of 110 bar using an intercooled compression train. A first compressor is used to compress the CO_2 from the second flash tank to the pressure at which the first flash tank is operating. Two more compressors and a pump are used to arrive at the final delivery pressure. After the first compression step, the CO_2 stream is cooled down to a temperature of 40 °C, which causes most of the water and all of the PZ to condense. This condensate stream is fed to the top of the absorber. An additional flue gas cooling step is present after the absorber in order to limit the PZ losses and control the water balance of the process. A make-up stream is used to add the same amount of water and PZ to the process as the amounts that are leaving via the flue gas and the pressurized CO_2 stream.

2.3. Model and computational issues

The capture plant is modelled using the simulation software Aspen Plus V8. A default template provided by the software vendor is used as basis for the simulation: 'ENRTL-RK_Rate_Based_PZ_Model.apwz'. This file contains relevant data on components, thermodynamic and transport properties, and reaction chemistry and rates. More details on the parameters used for the process and all process units are given in the following sections. Process unit input data is based on the recommendations from the European Benchmarking Task Force (EBTF, 2011).

2.3.1. Direct contact cooler

The direct contact cooler is a separation column where the temperature of the flue gas is reduced to 40 °C using direct countercurrent contact with cooling water at a temperature of 30 °C. The cooling water temperature is fixed and its flow rate is used to obtain the desired flue gas outlet temperature. Water that is accumulating in the cooling water circuit due to the decreasing vapour pressure in the flue gas is continuously being removed using a bleed stream. The column is simulated using four equilibrium stages and a fixed top pressure of 1.010 bar. A blower is used to increase the flue gas pressure to 1.040 bar to overcome the pressure drop in the downstream absorber. For the flue gas blower, isentropic and driver efficiencies of 0.75 and 0.95 are assumed.

2.3.2. Absorber

The absorber treats 770 kg/s of saturated flue gases with 14.08 mol% of CO_2 on a wet basis. It is simulated by a rate-based approach, using a mixed flow model and chemical reactions in the liquid film. Three sections of structured packing are used in the absorber. The height for all of them is 5 m and each one is discretized into 20 height elements of 25 cm. The top and bottom sections are equipped with Mellapak 250X packing, while the middle section contains 125X packing. This more open packing is used to accommodate the higher liquid flow rate in the middle section, related to the intercooling pump-around that is used. This pump-around extracts liquid from the bottom of the middle section, cools it to 40 °C, and returns it to the top of the middle section. A pump-around flow rate three times larger than the flow rate of the lean solvent is used. A flash unit at 43 °C is used to represent the flue gas cooling step after the absorber. A pressure drop of approximately 1.5 mbar/m was assumed, resulting in a final flue gas outlet pressure of 1.016 bar. The lean PZ solution enters the column with a CO_2 loading of approximately 0.31, expressed as mol CO_2 per mol of amine group (PZ has two amine groups per molecule). The loaded rich solution leaves the absorber with a loading of approximately 0.40. The exact value of the rich loading depends on the process conditions. To ensure that no solids are formed above a temperature of 0 °C, the CO_2 loading should be between 0.31 and 0.44 (Freeman et al., 2010a). The flow rate of the lean PZ solution is controlled to ensure that 90% of the entering CO_2 is absorbed.

2.3.3. Recuperative heat exchangers

The recuperative heat exchangers are used to preheat the rich solvent by cooling the lean solvent from the low pressure flash. The heat exchange process is divided into two sections. The colder section is modelled by keeping a temperature difference of 5 °C at both ends. In this section, the entire flow rate of cold rich solvent is always processed, since the rich solvent bypass split is downstream this section. In the hotter section, the cold stream outlet temperature is calculated from the thermal balance and varies according to the portion of by-passed rich solvent as further discussed in Section 3. The total pressure drop over both the exchangers is assumed to be 2 bar.

2.3.4. Flash tanks

Each of two flash tanks is modelled using two units of the flash models in the process simulator; the first is for the purpose

Table 2
Main assumptions for the calculation of the reference power plant.

Pulverized coal boiler	
Heat input, MW_{LHV}	1657.1
Primary/secondary air, %	25/75
Pressure losses in air preheater (each side), kPa	1
Pressure losses in mills and burners (I air), kPa	6.3
Pressure losses in windbox and burners (II air), kPa	3.3
Pressure losses in convective pass, SCR and FF, kPa	3.5
Pressure losses in FGD, kPa	2
Pressure losses in FGD gas–gas heater (each side), kPa	1
Furnace pressure, bar	1.01
Losses for radiation and unconverted C, %$_{LHV}$	0.35
Heat loss in heat exchangers, % of heat transferred	0.5
Oxygen concentration in flue gas at boiler exit, %vol.	2.9
Air in-leakages in the boiler, wt% of flue gas	1
Air in-leakages at FF, wt% of flue gas	5
Gas temperature at economizer outlet, °C	350
Hot gas temperature at air preheater outlet, °C	120
Boiler auxiliaries	
Fans isentropic efficiency, %	80
Fans electric-mechanical efficiency, %	94
Coal handling and milling, kJ_e/kg_{coal}	50
Ash handling systems, kJ_e/kg_{ash}	200
Flue gas desulfurization, kJ_e/kg_{SO_2}	5340
Miscellaneous BOP, % of input LHV	0.15
Steam cycle	
Boiler feedwater pressure, bar	320
Live steam temperature SH/RH, °C	600/620
Live steam pressure SH/RH, °C	270/60
SH/RH piping thermal losses, °C	2
SH/RH steam pressure losses at turbine inlet valve, %	2
RH steam pressure loss, bar	4
Condensing pressure, bar	0.048
Number of LP/HP preheaters	4/5
Pressure of steam bled for feedwater preheaters, bar	93.8/64.0/39.2/23.7/
	14.6/6.7/3.5/1.26/0.32
Pinch-point ΔT in preheaters, °C	3
Steam pressure losses in deaerator/HP preheaters, %	7/3
Feedwater pump hydraulic efficiency, %	85
Feedwater pump mechanical/electric efficiency, %	98.5/95
Auxiliaries for heat rejection to environment, kJ_e/kJ_{th}	0.008
Steam turbine	
Rotational speed, RPM	3000
Number of HP/IP/LP parallel flows	1/1/4
Crossover pressure, bar	5.2
Isentropic efficiency, %	Calculated
Last stage turbine blade height, m	1.04
Last stage peripheral velocity at mean diameter, m/s	500
Last stage exhaust area (per flow), m^2	10.4
Exhaust steam velocity, m/s	220
Steam turbine mechanical efficiency, %	99.6
Electric generator efficiency, %	98.5

of simulating the heating part of the flash, and the second is for the purpose of simulating the packed section of the flash tank. A variable amount of rich solution is by-passing the hot section of the heat exchanger and fed to the top of the packed sections of each flash tank. The pressure of the second flash tank is determined by the desired lean loading of the regenerated solvent. It is found by requiring that the amount of CO_2 that is leaving the process is exactly the same as the amount that is being absorbed. The pressures of both flashes are used as optimization variables for the process.

2.3.5. CO_2 compression

After the first compression under moderate pressure ratio of the CO_2 released from the LP flash up to the HP flash pressure, the entire CO_2 released from the capture section is dried to reach the specifications of the transport pipeline. Instead of including this first compression stage, throttling the CO_2 from the HP flash to the LP flash pressure might be a preferable option on an economic basis. This option, which would inevitably reduce the benefits of the

two-stage regeneration process and lead to lower thermodynamic performance, is however not assessed in this work.

The high purity (>99.9%) CO_2 from the flashes is then compressed by an intercooled two-stage compression train up to 80 bar and then pumped up to 110 bar at liquid state. The total pressure ratio of CO_2 compression, which is equally divided between the two stages, changes when the HP flash pressure is changed. The CO_2 compressors and the CO_2 pump are driven by electric motors and are modelled with isentropic efficiencies of 0.80 and 0.75 and mechanical–electric efficiencies of 0.95 and 0.92, respectively. In the intercooler, CO_2 is cooled down to 35 °C. In the after-cooler, CO_2 is cooled to 25 °C before the final pumping. Both the intercooler and after-cooler steps are divided into two sub-steps; a first sub-step ending at 42 °C, where heat is recovered for integration with the power plant by the condensate from the steam cycle condenser, and a second sub-step where low quality heat is rejected using cooling water. Only the first sub-steps are shown in Fig. 2. The Peng–Robinson equation of state with the default Aspen Plus coefficient has been used to calculate CO_2 compression.

2.3.6. Integration with the power plant

The configuration of the power plant with CO_2 capture by the PZ-based process (Fig. 2) is shown in Fig. 3. The same layout and operating parameters of the reference plant without CO_2 capture have been maintained for all the units upstream of the FGD. After desulfurization, gas is further cooled in a DCC and then enters the CO_2 absorber of the PZ process. Heat for solvent regeneration, indicated by purple arrows numbered 1 in Figs. 2 and 3, is provided by LP steam taken from steam turbine crossover, whose pressure is set at 6.7 bar. Considering a pressure drop of 0.5 bar, steam is condensed in the heat exchangers of the flash tanks at 6.2 bar and 160 °C, assuring in this way a minimum temperature difference of 10 °C between the condensing steam and the solvent. Since steam extracted from the crossover is at a temperature of around 290 °C, it is conditioned by attemperation with liquid water to 180 °C in order to avoid solvent degradation due to high tube skin temperatures. For attemperation, a small fraction of condensate from the regenerative flash tanks is recycled, with negligible effects on power plant performance, only associated to a small pumping consumption.

Another point to be considered is that the pressure of the steam used for solvent regeneration is lower than the pressure of the two flash tanks. This means that measures to avoid leakage of solvent in the water circuit (e.g. an intermediate water loop at higher pressure) are needed to avoid risks of contamination of the water returned to the steam cycle in case of tubes failure.

A large portion of the water from the steam cycle condenser is also sent to the CO_2 absorption and compression units to recover low temperature heat from flash vapour cooling and CO_2 compressors intercoolers. Warm water is produced from these two sources, keeping a minimum temperature difference of 10 °C also in these heat exchangers. This water is then returned to the steam cycle in the deaerator and/or in the water preheater line. The temperature of the water produced by cooling flash vapours and compressed CO_2 varies depending on the process parameters. Temperatures between 120 and 140 °C are obtained from flash vapour cooling, depending on the flash vapour temperature. These heat streams are indicated by purple arrows numbered 2 in Figs. 2 and 3. The temperature of the water heated by CO_2 cooling varies between 96 and 126 °C in the cases considered in this work, depending on the pressure ratio of the CO_2 compressors. These heat streams are indicated by purple arrows numbered 3 in Figs. 2 and 3. In particular, since CO_2 is always compressed in two intercooled stages, compression ratio and hence CO_2 temperature at intercooler and aftercooler inlet increases when the HP flash pressure is reduced.

When the temperature of the two water streams differs by more than 20 °C, two separate lines returning to the steam cycle have
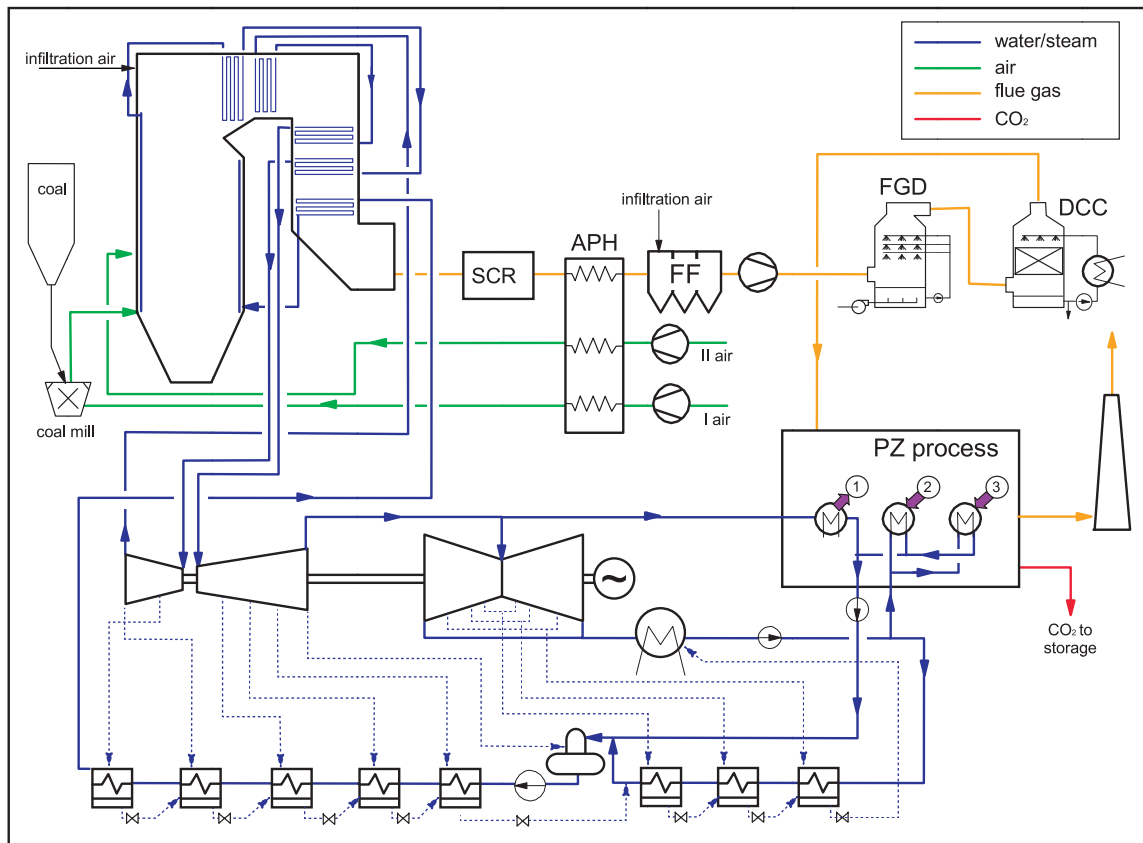
Fig. 3. Schematic of the power plant with CO_2 capture by PZ process.

been considered. The hottest one, produced from flash vapour cooling, is returned to the deaerator after mixing with the condensate at 160 °C of the steam used for solvent regeneration. The coldest water is instead preheated in a surface regenerator before being sent to the deaerator. In some cases, for HP flash pressures below about 13 bar, a single water flow is returned to the deaerator. This last condition, which occurs in the optimal cases from the sensitivity analysis, is shown in Fig. 3.

Due to the reduced steam flow rate in the LP section, a double-flow turbine is adopted in the capture cases. In the sensitivity analysis, the blade height of the last stage is adapted to keep an exhaust velocity of 220 m/s, maintaining the same leaving losses of the reference case. In the optimal thermodynamic case calculated in this work, which is the case with the minimum heat duty for flash regeneration and hence the maximum flow rate expanded in the LP turbine section, the target exhaust velocity is obtained with a turbine exhaust area slightly below 16 m² per flow, which corresponds to the largest section for 50 Hz machines offered by Siemens (Leyzerovich, 2007). Of course, the number of parallel LP flows and the last stage size depend on the size of the plant and will change for a plant with a larger heat input.

Table 3 gives the main input values used for simulation of the CO_2 capture plant and its integration with the power plant.

2.4. Definition of simulation cases

The sensitivity of the process performance to changes in several capture plant operating conditions is investigated as part of this study. The four assessed properties are the pressures of the two flash tanks ($p_{HP\text{-}FL}$ and $p_{LP\text{-}FL}$), the temperature drop of the flash vapour in the washing section (ΔT_{ws}) due to cold rich by-pass, and the temperature difference at the ends of the recuperative heat exchanger (ΔT_{HE}).

The LP flash pressure is directly linked to the lean solvent loading, since the regeneration temperature is kept constant at 150 °C. A minimum lean loading of 0.30 has been selected to avoid solids formation at low temperature, which constrains a minimum LP flash pressure of 9.51 bar.

2.5. Reference capture plant

During the Cesar project, some process modifications were tested at the pilot plant at Esbjerg in Denmark. As reported by Knudsen et al. (2011), the effect of employing Lean Vapour Compression (LVC, see Fig. 4) was very promising with respect to reduced steam consumptions for an MEA based solvent system. This reference capture plant is used in the present study to benchmark the piperazine based process. The same modelling approach and simulation software is used for both processes.

Table 4 shows the main input values used for simulation of the MEA reference capture plant that are different from or additional to the values used for the PZ-based process as given in Table 2.

The benchmark MEA process was integrated in the power plant with the same criteria as used for the PZ cases. Heat for the stripper reboiler, as indicated with the purple arrows numbered 1 in Fig. 4, is provided by steam extracted from the turbine crossover, whose pressure is reduced to 3.3 bar, to keep the minimum temperature difference of 10 °C between the condensate and the lean solvent. Heat recovery from the stripper condenser, as indicated with the purple arrows numbered 3 in Fig. 4, was included too, allowing to preheat a part of the boiler feed-water to 90 °C. Also in this case, heat from the CO_2 compressor intercoolers is recovered by preheating a portion of the condensate from the steam cycle condenser, as indicated with the purple arrows numbered 2 in Fig. 4. Three intercooled CO_2 compressor sections have been assumed, allowing for preheating the water to 140 °C. It was demonstrated

Table 3
Main assumptions for the simulation of the CO_2 capture plant and its integration with the power plant.

Direct contact cooler	
Flue gas outlet temperature, °C	40
Water inlet temperature, °C	30
Contactor pressure drop, mbar	30
Number of contactor equilibrium stages	4
Flue gas blower isentropic efficiency, %	75
Flue gas blower driver efficiency, %	95
Pump isentropic efficiency, %	80
Pump driver efficiency, %	95
Absorber	
Concentration PZ, wt%	40
Lean solvent inlet temperature, °C	40
Packing height top/middle/bottom sections, m	5/5/5
Packing type top/middle/bottom sections, Mellapak	250X/125X/250X
Pump-around inlet temperature, °C	40
Pump-around flow-rate, % of the lean solvent flow	300
Water wash gas outlet temperature, °C	43
Maximum vapour capacity, % of flooding	70
CO_2 capture efficiency, %	90
Pressure drop, mbar/m	1.5
Recuperative heat exchangers	
Temperature difference between cold inlet and hot outlet, °C	5
Total pressure drop, bar	2
Regenerative flash tanks	
Heating temperature, °C	150
Number of water wash equilibrium stages	1
CO_2 compression	
CO_2 compressor isentropic efficiency, %	80
CO_2 compressor driver efficiency, %	95
CO_2 compressor stages (incl. LP to HP)	3
CO_2 compression intercooling temperature, °C	35
CO_2 compression after-cooling temperature, °C	25
CO_2 pump isentropic efficiency, %	75
CO_2 pump driver efficiency, %	92
CO_2 pumping pressure start/delivery, bar	80/110
Power plant integration	
Steam withdrawal pressure, bar	6.7
Steam pressure drop, bar	0.5
Minimum temperature difference for flash heating, °C	10
Maximum steam temperature for flash heating, °C	180
Minimum temperature difference for heat recovery, °C	10

Table 4
Main assumptions for the simulation of the CO_2 capture plant using 30 wt% MEA and lean-vapour compression.

|	
Absorber	
Concentration MEA, wt%	30
Packing height, m	12.5
Packing type, Mellapak	2X
Water wash liquid inlet temperature, °C	42
Regenerator	
Packing height, m	10
Packing type, Mellapak	2X
Maximum vapour capacity, % of flooding	70
Heating temperature, °C	120.7
Regenerator pressure, bar	1.91
Flash pressure, bar	1.10
CO_2 compression	
CO_2 compressor stages	3
Power plant integration	
Steam withdrawal pressure, bar	3.3

in other studies (Pfaff et al., 2010) and verified in this work that a larger number of compression stages leads to a lower electric consumption for CO_2 compression but also to lower overall plant efficiencies due to the lower amount and the lower quality of the heat recovered. The preheated water from the CO_2 intercoolers is mixed with the condensate from the MEA stripper and returned to the deaerator. The intercooling steps are again divided in two sub-steps: a heat recovery step integrated with the power plant, and a heat rejection step using cooling water.
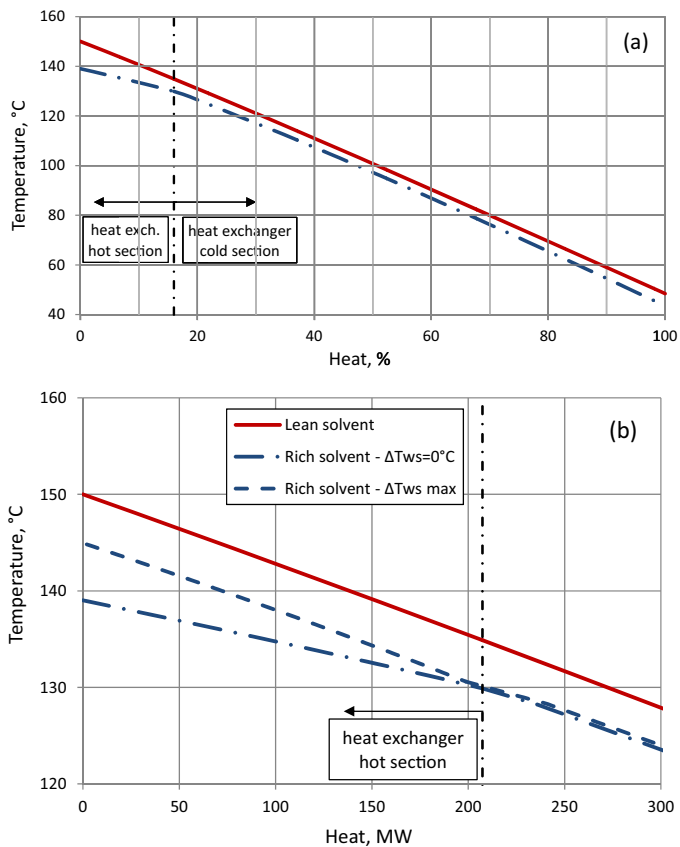
3. Results and discussion

3.1. LP flash pressure and flash vapour temperature drop

In this section, the effects of the LP flash pressure ($p_{LP\text{-}FL}$) and of the temperature drop of the flash vapour in the washing section (ΔT_{ws}) on plant performance are presented. Reference values for the HP flash pressure of 16 bar and for the temperature difference at the recuperative heat exchanger of 5 °C are kept in all the simulations presented in this section.

The target ΔT_{ws} has been obtained in each case by tuning the cold-rich by-pass fraction to each flash tank. A maximum by-pass fraction (and hence a maximum ΔT_{ws}) exists as a result of the temperature profile inside the recuperative heat exchanger. This can be explained through Fig. 5, where temperature–heat diagrams are
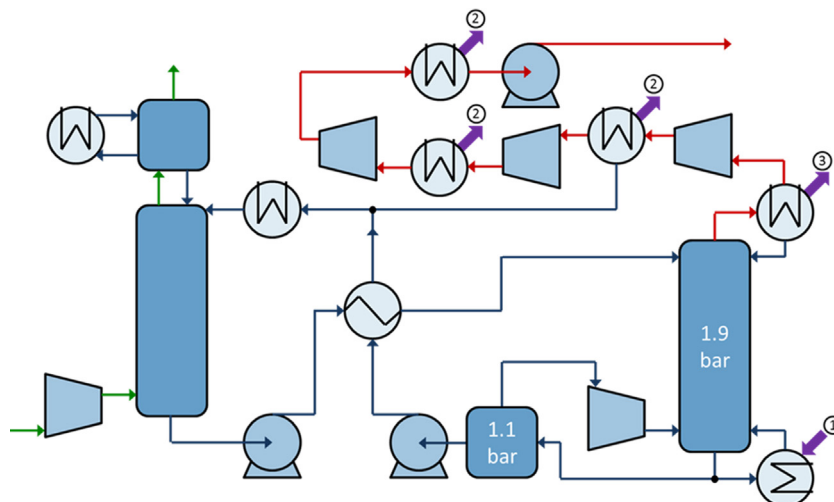
Fig. 4. Flowsheet of a CO_2 capture plant with the lean vapour recompression (LVC) configuration.

Fig. 6. Lean solvent circulation and total steam evaporated in the flashes per kg of CO_2 captured for different LP flash pressures and ΔT_{ws}.
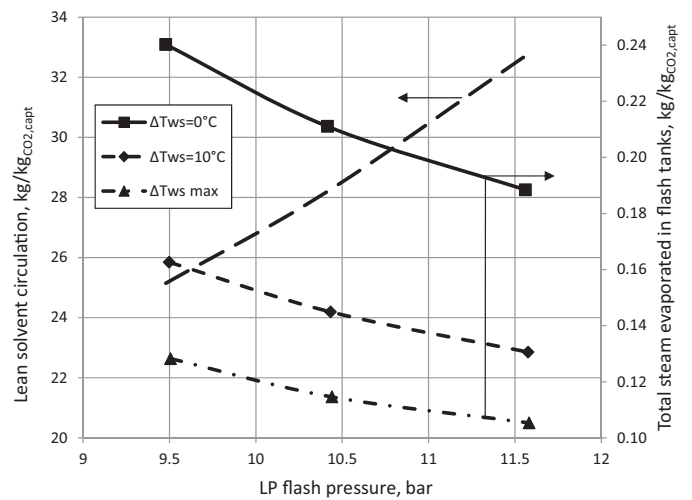
Fig. 5. Temperature–heat diagram of the recuperative heat exchanger of a representative case with no rich solvent by-pass (a) and detail of the hot section of the of the cases with no rich solvent by-pass and maximum by-pass (b).

reported. In Fig. 5a, the complete diagram of a case with no rich solvent split (i.e. $\Delta T_{ws} = 0$) is shown. In the colder section of the heat exchanger, the minimum ΔT of 5 °C at the two ends is kept, which leads to a minimum internal ΔT of about 3.1 °C due to variable specific heat of the two streams (especially of the rich solvent) with temperature. At the temperature of about 130 °C the bubble point of the rich solvent is reached and the heat capacity of the rich solvent increases. As a consequence, ΔT increases leading to a temperature difference at the hot end of the heat exchanger of about 11 °C.

In Fig. 5b, the hotter section of the case just described with no solvent split is shown more in details (cold stream in dash-dotted line) and compared to a case with the maximum split fraction of around 42% (cold stream in dashed line). Considering this second case, it is shown that the increase of the heat capacity of the cold stream in the hotter section due to vapour phase formation is balanced by the lower flow rate of cold rich solvent. Therefore, the curves are parallel in this section and a temperature difference of 5 °C can be kept also at the hot end of the heat exchanger. It is clear that higher cold rich solvent by-pass fractions are not possible without reducing the ΔT in the heat exchanger below the target value of 5 °C, or by increasing the ΔT in the colder section of the heat exchanger (and ultimately reducing the heat recovered) with detrimental effects on process efficiency. Therefore, this condition represents the maximum split fraction, which leads to a maximum ΔT_{ws} of around 20 °C in all the cases assessed.

The heat requirements in the two flash tanks are caused by three contributions: (i) the sensible heat to heat the solvent up to the regeneration temperature, (ii) the latent heat to evaporate the water vapour in the flash tanks and (iii) the heat of reaction between CO_2 and the solvent. Since a constant CO_2 capture rate is

kept, the contribution of the heat of reaction is constant in all the cases. The other two contributions have opposite trends when the LP flash pressure is changed. This is shown in Fig. 6, where the total steam evaporated in the two flash tanks and the lean solvent circulation rate per kg of CO_2 captured are reported. From this figure, it can be observed that when the LP flash pressure is increased, a lower amount of steam is evaporated, since the equilibrium partial pressure of H_2O in the vapour phase is obtained with a lower H_2O concentration thanks to the higher absolute pressure. On the other hand, the loading of the lean solvent increases, leading to higher circulation rates needed to absorb the target CO_2 flow rate.

As also shown in Fig. 6, the rich cold solvent by-pass has no effect on the lean solvent circulation. This results from the fact that the lean solvent loading depends only on the flash tank temperature and pressure. Conversely, increasing the rich cold solvent by-pass reduces the steam flow rate released from the flash tanks, since a higher ΔT_{ws} results in a larger portion of steam to be condensed in the washing section.

The effects on the total heat duty in the flash tanks are shown in Fig. 7. As a result of the opposite trends discussed previously, the curves at constant ΔT_{ws} show a minimum. Due to the reduced amount of steam exported with the stripped CO_2, when ΔT_{ws} is increased the total heat duty reduces considerably (by about 10% from $\Delta T_{ws} = 0$ °C to the maximum ΔT_{ws}) and the minimum heat duty is obtained for lower LP flash pressures. Actually, for ΔT_{ws} of 10 °C or higher, the minimum heat duty is obtained at
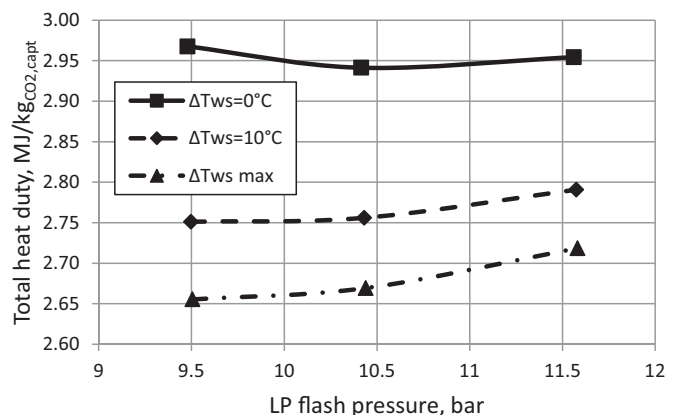
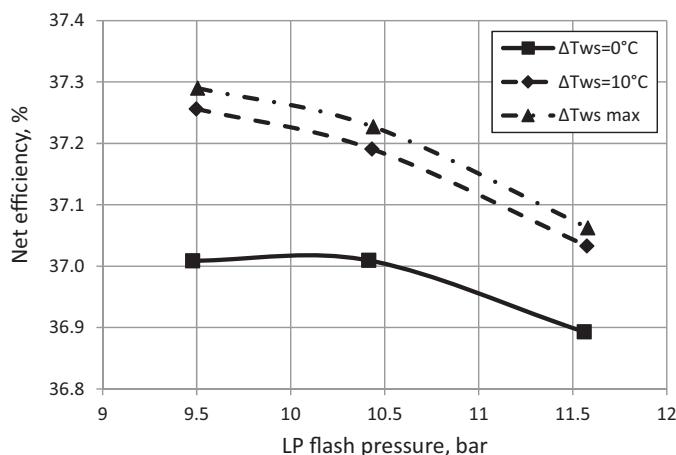**Fig. 7.** Specific heat duty in the flashes for different LP flash pressures and ΔT_{ws}.

Fig. 8. Net plant efficiency as function of the LP flash pressure and ΔT_{ws}.

Fig. 9. Total steam evaporated in the flashes and total heat duty as function of the HP flash pressure.

flash pressures lower than the minimum of 9.51 bar considered. As evident from the figure, very small improvements are however obtainable by reducing the LP flash pressure even further.

In the optimal thermodynamic case, a heat duty of about 2.65 MJ/kg$_{CO_2\text{-capt}}$ has been obtained. This value is in the lower range of the energy requirements reported in the literature for many solvent systems (Singh et al., 2013) and about 20% lower than the benchmark MEA process considered in this study.

The effects on the net plant efficiency are finally reported in Fig. 8. The trends of the curves basically reflect the total heat duty of the flash regenerators shown in Fig. 7 and a maximum efficiency exists for each ΔT_{ws}. Also in this case, when ΔT_{ws} of 10 °C or higher are selected, the thermodynamic optimal flash pressure seems lower than the minimum value considered for avoiding solids formation at low temperature. However, from the slope of these curves, it is expected that only minor improvements would be obtained by reducing the LP flash pressure further.

3.2. HP flash pressure

The third parameter assessed in the sensitivity analysis is the pressure of the high pressure flash. Considering the outcomes of the previous analysis, the LP flash pressure has been kept at the minimum value of 9.5 bar, corresponding to a lean solvent loading of 0.30 mol of CO_2 per mol of amine group. Also the ΔT_{ws} has been kept equal to the maximum value allowed in each case. The pressure of the HP flash has been varied between 9.5 and 17 bar. The lower limit is clearly constrained by the LP flash pressure and implies a single flash configuration.

In Fig. 9, the total steam evaporated and the total heat duty are reported for different HP flash pressures. In general, when the HP flash pressure is increased, a lower amount of water is evaporated in the HP flash. On the other hand, an increasing amount of CO_2 is stripped in the LP flash and hence also an increasing amount of steam is generated in the LP flash, in accordance with the H_2O concentration in the vapour phase determined by the vapour–liquid equilibrium. As a result, a minimum at about 12.5 bar is obtained for the total steam evaporated in the two flash tanks.

Since the HP flash pressure does not influence the CO_2 loading in the lean solvent and hence the solvent circulation rate, the sensible heat to heat the solvent up to the regeneration temperature is not affected by HP flash pressure. Therefore, the heat duty variation reflects the need of latent heat for steam evaporation and also the minimum heat duty is obtained for a pressure of 12.5 bar.

It must be highlighted that the variations of heat duty are rather small (about 1% in the range assessed). As a consequence, also the
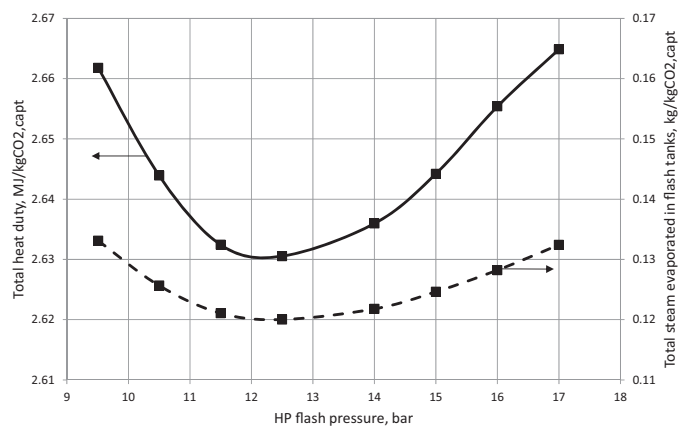
net electric efficiency is not very sensitive to the HP flash pressure. This is shown in Fig. 10, where variations of less than 0.1% have been obtained by varying the HP flash pressure between 9.5 and 16 bar. In order to confirm that the optimal LP flash pressure remains at 9.5 bar when changing the HP flash pressure, also a case with LP and HP flash pressures of 10.0 and 12.5 bar has been assessed. It was indeed found the net electric efficiency decreased for this case, compared to the optimal case obtained for LP flash pressure of 9.5 and HP flash pressure of 12.5 bar.

3.3. Minimum temperature difference in the recuperative heat exchanger

The final parameter assessed in the sensitivity analysis is the ΔT at the ends of the recuperative heat exchanger. The optimal value of this parameter will result from an economic analysis, which is beyond the scope on this work. As a matter of fact, by increasing the ΔT, lower investment costs for the recuperative heat exchanger will be possible. On the other hand, higher heat duties and hence higher operating costs will also result.

The effects of the ΔT on net plant efficiency and on the combined heat transfer coefficient (U) and the heat exchanger area (A) of the recuperative heat exchanger and the heat exchangers in the flashes are shown in Fig. 11. The operating parameters of the PZ-opt case have been kept in this analysis. By increasing the ΔT from 5 to 10 °C, the UA reduces by about 50%. A further increase of the ΔT up to 15 °C leads to a reduction of UA of 65% with respect to the base case. On the other hand, a linear trend is obtained for the plant
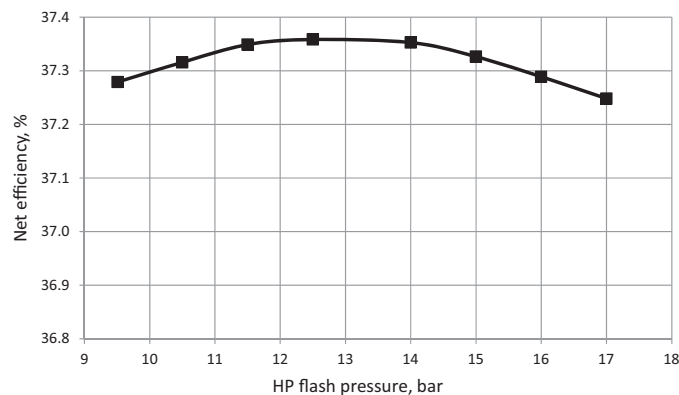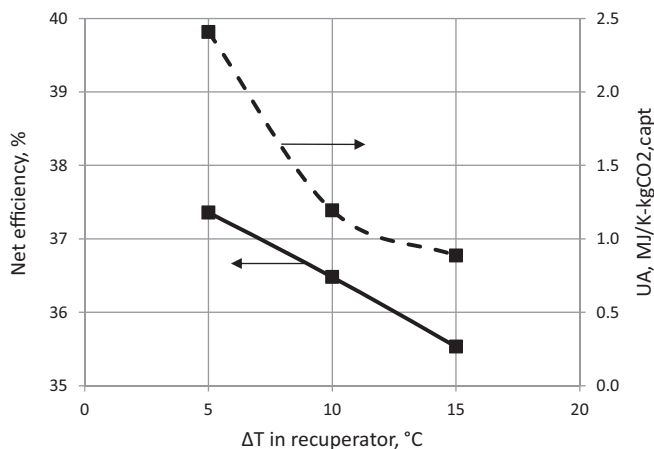

Fig. 10. Net plant efficiency as function of the HP flash pressure (the same scale of Fig. 8 has been used for the efficiency axis, to highlight the limited influence of the HP flash pressure).

Fig. 11. Net plant efficiency and UA of the recuperative heat exchanger and the heat exchangers in the flashes as function of the ΔT at the ends of the recuperative heat exchanger.

electric efficiency, with a reduction of almost 1% point for each 5 °C of increase of the ΔT.

3.4. Overall performance comparison

The detailed power balances of the most interesting cases assessed in this sensitivity analysis are reported in Table 5. In the first column, the balance of the reference plant with no CO_2 capture is reported. A net electric efficiency of 44.6% is obtained, with specific CO_2 emissions of 782 g/kWh. In the second column the results of the simulation of the benchmark plant with CO_2 capture by an MEA-based process are resumed. A net electric efficiency of 35.5% has been calculated, corresponding to a penalty of 9.1% with respect to the plant with no CO_2 capture.

Three of the piperazine-based cases assessed in this work are reported in the last three columns. The reference case (PZ-ref) refers to the case with cold rich solvent split fractions of 2.5% and 5.0% to the HP and LP flashes respectively, as proposed by Frailie et al. (2013). Pressures of the flashes are set to 16 and 10.4 bar, based on the results from an exploratory study on the integration between a power plant and piperazine-based capture plant by Van der Ham et al. (2013). The net efficiency obtained for this case is 37.2%, about 7.4% less than the reference case and 1.8% higher than the MEA-based plant. The resulting specific CO_2 emission in this case is 93.8 g/kWh, corresponding to 88% of CO_2 avoided. The optimal case (PZ-opt) refers to the optimal thermodynamic plant, i.e. with the minimum LP flash pressure of 9.5 bar, the maximum ΔT_{ws} of about 20 °C and the optimal HP flash pressure of 12.5 bar. An efficiency increase of 0.2% is obtained with respect to the PZ-ref case, also leading to minor improvements of specific CO_2 emissions which decrease to 93.2 g/kWh. The last case shown in Table 5 is the single flash case (PZ-1FL). The efficiency of this case decreases by less than 0.1% with respect to the PZ-opt case. This result makes this case very interesting and potentially superior to the two-flash configuration from a techno-economic point of view, due to the simpler layout and the avoidance of one pressurized tank and of the compressor of the CO_2 released from the LP flash.

The differences in the power balance among the PZ cases lie in the gross electric power, which is directly related to the heat duty and in different share of auxiliaries consumption of the CO_2 capture section. Among the cases reported in Table 5, the consumption of the solvent pump and of the CO_2 compressors vary. Solvent pump power increases by increasing the solvent flow rate and the pressure increase. Therefore, the case with the highest LP flash pressure (PZ-ref case), and hence the highest lean solvent loading, shows the

maximum solvent pump consumption. The PZ-opt case has the second highest pump consumption, since rich solvent is compressed up to 12.5 bar, vs. 9.5 bar of the PZ-1FL case, keeping in mind that the solvent circulation rate is the same for these two cases. An opposite trend is obtained for the CO_2 compressors: the higher the pressure of the two flash tanks, the lower the compression power.

With respect to the benchmark MEA-based plant, similar steam turbine power outputs and gross efficiencies have been obtained despite the lower flow rate of the steam bled for solvent regeneration. This is due to the lower pressure of the bled steam and the good quality of the heat recovered from the CO_2 compression section in the MEA case. The reason of the higher PZ plants efficiencies is hence the lower auxiliary consumption. The main difference is associated with the much lower electric consumptions for CO_2 compression of the PZ plants as a consequence of the high pressure solvent regeneration. This is obtained with a higher consumption of the solvent pump, which has to compress the solvent to higher pressures. However, this is more than balanced by the power absorbed by the lean vapour compressor in the MEA case.

The net efficiency and the specific emissions of the plants can be evaluated jointly by means of the specific primary energy for CO_2 avoided (SPECCA) index, defined as in Eq. (1) (EBTF, 2011):

$$\text{SPECCA} = \frac{3600 \cdot ((1/\eta_{el}) - (1/\eta_{el,ref}))}{E_{CO_2,ref} - E_{CO_2}} \tag{1}$$

Values around 2.3 MJ/kg$_{CO_2}$ have been obtained for the PZ plants, a very favourable result compared to the competitive MEA-based case, showing a SPECCA higher than 3.0 MJ/kg$_{CO_2}$.

4. Considerations on part-load operations and plant flexibility

Among the strategies to improve flexibility, rich and lean solvent storage is one of the most promising options to avoid CO_2 emission during start-ups, to allow increased power production during peak hours and as buffer to reduce variations of CO_2 flow rate to the pipeline in case of load following. As a matter of fact, by including vessels for rich and lean solvent storage, it is possible to operate the capture plant decoupled from the power plant. This is useful for example during start-ups, when steam at sufficient pressure for solvent regeneration is not available for durations of the order of hours and stored lean solvent, produced when steam for regeneration is available, can be used for CO_2 capture. Solvent storage can also be employed to increase the revenues from plant operations, reducing the steam extraction during peak hours at high electricity price and capturing the CO_2 by means of stored lean solvent, produced during off-peak hours with low electricity price by extra steam extraction. Finally, rich solvent can be used as a temporary CO_2 storage system in case of cycling operations, allowing to deliver a constant CO_2 flow rate to the compression section and to the pipeline. In all the cases, the optimal design and operation strategy will depend on an economic trade-off, depending on the increased revenues from electricity trading, on the value of the carbon tax and on the cost of the equipment both for the additional storage tanks and for the possible oversizing of other components.

In any case, the cost of the storage tanks will depend on their size, on the design pressure and on the construction material. As far as storage tanks volume is concerned, the volume of solvent needed to absorb one kg of CO_2 is the parameter to be taken into account in a comparative analysis. According to the Aspen Plus thermodynamic model, MEA based plants seem advantaged, requiring a lower volume of solvent to capture one kg of CO_2 (15 l vs. 22–25 l for the PZ cases). On the other hand, since according to Gunasekaran et al. (2013) a PZ based solvent is less corrosive than MEA, a cheaper vessels material may be used in PZ based plants.

Table 5
Power balance of selected cases, compared to reference plant without CO_2 capture and a reference plant with MEA-based CO_2 capture.

Name of the configuration	Ref no-capt	MEA	PZ-ref	PZ-opt	PZ-1FL
CO_2 capture	No	Yes	Yes	Yes	Yes
HP/LP flash pressure, bar	–	–	16/10.4	12.5/9.5	9.5
Cold rich split fraction to HP/LP flash, %	–	–	2.5/5	23/19	42
ΔT in HP/LP flash washing section, °C	–	–	11.5/7.2	20	22.4
Heat duty, $MJ/kg_{CO_2,capt}$	–	3.29	2.76	2.63	2.66
Lean solvent circulation rate, $kg/kg_{CO_2,capt}$	–	16.2	28.2	25.1	25.1
Lean solvent circulation rate, $1/kg_{CO_2,capt}$	–	15.5	25.3	22.5	22.5
Electric power balance, MW_e					
Steam turbine	795.5	705.4	703.5	706.7	707.3
Boiler feedwater pump	−25.94	−25.93	−25.93	−25.93	−25.93
Condensate extraction pump	−0.63	−0.59	−0.51	−0.52	−0.53
Condenser auxiliaries	−6.18	−3.73	−4.45	−4.52	−4.55
Auxiliaries for heat rejection (other than cond.)	–	−3.21	−1.28	−1.19	−1.64
Coal milling and handling	−3.29	−3.29	−3.29	−3.29	−3.29
Filters and ash handling	−1.86	−1.86	−1.86	−1.86	−1.86
Flue gas desulfurizer	−3.29	−3.29	−3.29	−3.29	−3.29
I air forced draft fan	−1.25	−1.25	−1.25	−1.25	−1.25
II air forced draft fan	−2.17	−2.17	−2.17	−2.17	−2.17
Induced draft fan	−9.86	−9.86	−9.86	−9.86	−9.86
CO_2 absorption tower flue gas blower	–	−2.78	−2.78	−2.78	−2.78
Solvent pump	–	−1.71	−8.17	−5.80	−4.51
Lean vapour compressor	–	−8.18	–	–	–
CO_2 compression	–	−47.05	−20.21	−22.70	−25.34
BOP	−2.49	−2.49	−2.49	−2.49	−2.49
Net electric plant output, MW_e	738.6	588.0	615.9	619.1	617.8
Coal input, kg/s	65.84	65.84	65.84	65.84	65.84
Coal thermal input, MW_{LHV}	1657.1	1657.1	1657.1	1657.1	1657.1
Boiler efficiency, $\%_{LHV}$	94.1	94.1	94.1	94.1	94.1
Gross electric efficiency, $\%_{LHV}$	48.01	42.57	42.45	42.65	42.68
Net electric efficiency, $\%_{LHV}$	44.57	35.48	37.17	37.36	37.28
Net electric efficiency penalty, points $\%_{LHV}$	–	9.09	7.40	7.21	7.29
Carbon capture ratio, %	0	90.0	90.0	90.0	90.0
CO_2 specific emission, g/kWh	782.1	98.2	93.8	93.3	93.5
CO_2 avoided, %	–	87.4	88.0	88.1	88.0
SPECCA, MJ/kg_{CO_2}	–	3.02	2.34	2.26	2.29

When operating at part load or following any flexibility criteria leading to off-design operations, the effects of variable steam flow rates on steam extraction pressure, on steam turbine efficiency and on the condensing pressure need to be considered. It must be said that steam turbines are flexible components, which can safely operate at loads of the order of 20–30% of the nominal one. However, when reducing the steam flow rate at the LP section admission, either because of part load operations or because of extra lean solvent production to be stored for use during peak hours, the pressure at the LP turbine inlet and the steam axial velocity along the expansion also reduce. One option to manage the pressure reduction is using a throttling valve at the LP section inlet to keep the crossover pressure at the nominal value even at reduced steam flow rates, so that steam for the capture section can be extracted at constant pressure even at part-load. Another option would be to accept a reduction of the steam pressure to the capture section, leading to lower regeneration temperatures. In this case, losses associated to steam throttling would be avoided, but a higher lean solvent loading would result, leading either to higher solvent circulations to keep a given capture rate, or reduced capture efficiencies, or reduced effectiveness of solvent storage volume.

The opposite condition might occur during peak hours, when steam flow rates higher than the design one could be expanded in the turbine to boost power generation and take advantage of the high electricity price. The limiting case is the one with no steam extraction, which could be possible in case of sufficient lean solvent storage volume or if the capture section is bypassed and the CO_2 is entirely vented. In this case, the increased steam flow in the LP turbine would lead to increased power output and crossover pressures. Therefore, crossover, LP steam turbine casing, shaft, electric generator and auxiliary systems should be designed for maximum

pressure and maximum power higher than the nominal one under CO_2 capture operations, with negative impact on the plant capital costs. The increased steam flow through the low pressure turbine would also lead to lower turbine efficiency due to increased losses associated to the residual kinetic energy of the steam discharged at higher velocity from the last stage. Under these conditions, the condensing pressure will also increase if additional cooling capacity for the condenser (i.e. oversizing of the condenser with respect to nominal operations with CO_2 capture) is not present, hence reducing the steam cycle efficiency. In any case, despite the fact that the plant can be properly designed to safely handle such steam flow rate increase, if operations with no CO_2 capture are expected for long periods, the installation of a parallel dedicated turbine to expand the extra steam with high efficiency is another option. Also in this case, the additional capital costs for the additional turbine and the related equipment should be considered.

While the optimal design strategy to manage flexible operations would require off-design calculations of both the power plant and the capture section, which are beyond the scope of this work, the different adaptability of steam turbines of power plants utilizing different solvent systems can be initially estimated by comparing the variation of steam flow rate in the LP turbine under design condition and under no-capture operation. This difference is directly linked to the heat duty for solvent regeneration at the design point and the PZ based process assessed is hence expected to be somewhat superior to the MEA one. In particular, the mass flow rate at the LP turbine inlet increases by 62% when no steam is directed to the PZ based process and conditions of the reference plant with no CO_2 capture are re-established, while it almost doubles in case of MEA. The mass flow reduction associated with steam extraction for water preheaters in the no-capture case, when no

low temperature waste heat is available from the capture section, helps reducing steam flow variations and is taken into account.

An important unit that can limit the flexibility of a capture plant is CO_2 compression. As a matter of fact, for high turn-down ratio compressors operations become inefficient (if recycle of compressed CO_2 is used to avoid compressor surging) or require additional equipment like variable speed drives or parallel compression units. The problems associated to CO_2 compression are reduced in the PZ based process with respect to all the systems with atmospheric pressure solvent regeneration. Since the regeneration takes place at relatively high pressure, a lower number of intercooled compressor stages can be used and power consumption at the design point is between 130 and 180 kJ_e/kg_{CO_2}, vs. 325 kJ_e/kg_{CO_2} of the MEA case. Therefore, the effect of inefficient operations will have a lower weight on the overall plant performance, or the relative contribution to capital cost would be smaller for the PZ-process in case of installation of additional equipment.

5. Conclusions

A concentrated piperazine (PZ) based post combustion capture process integrated with a power plant has been studied. In the regeneration part of the process, the stripper column is replaced by two flash tanks each operated at elevated pressure compared to the conventional stripper process. The energetic performance of the process is compared to the corresponding performance of a power plant without capture and to a benchmark MEA-based capture process. Both capture processes are integrated with the power plant in an optimal manner meaning that heat released through cooling is utilized and the conditions of the steam withdrawn from the power plant for the heat requirement of the reboiler is optimized.

A sensitivity analysis of the process performance to changes in several capture plant operating conditions is investigated as part of this study. The four assessed properties are the pressures of the two flash tanks, the temperature drop of the flash vapour in the washing section due to cold rich by-pass, and the temperature difference at the ends of the recuperative heat exchanger. It was found that the optimal pressure in the LP flash was 9.5 bar, which is the same as the minimum pressure to avoid solids formation at low temperature. However, any improvement below this value is only minor. Furthermore, it is concluded that the optimal cold-rich by-pass fraction is the one leading to the maximum temperature drop of the flash vapour in the washing section. This maximum temperature drop is limited by the target of $5\,°C$ ΔT for the hot end of the recuperative heat exchanger. For this optimal case, a heat duty of about 2.65 $MJ_e/kg_{CO_2\text{-capt}}$ has been determined. This value is in the lower range of the energy requirements reported in the literature for many solvent systems and about 20% lower than the benchmark MEA process. In addition, a significant decrease in CO_2 compression power has been obtained for the PZ process with respect to the MEA plant, due to the high regeneration pressure. The corresponding net efficiency obtained for the total power plant with the PZ-based capture process is 37.2%, which is 7.4% less than the reference power plant without CO_2 capture and 1.9% higher than the MEA case. With this optimal LP pressure fixed, the optimal HP pressure has been determined and the value is 12.5 bar. The improvement in the corresponding net efficiency is only 0.2%. With the optimal LP/HP pressures, the temperature difference at the ends of the recuperative heat exchanger has been varied and it is concluded that while the net efficiency will decrease with increasing ΔT, the heat exchanger area will decrease meaning lower capital costs. This is just one example of the trade-offs between operating costs (directly related to the efficiency loss) and the capital cost of the process equipment. Another example is the case, in

which only one flash tank was used with the same pressure as the LP flash tank (i.e. 9.5 bar). It is shown that the efficiency loss increases slightly (0.1%), but the capital cost will decrease. Thus in order to make a complete optimization, a thorough cost analysis is also required. However, this is beyond the scope of the present paper.

Finally, a more qualitative analysis has been made related to flexibility of the power plant operation and the effect on the capture plant. It seems that the PZ-based capture process is superior to the MEA-based benchmark process due to lower amount of extracted steam and lower energy consumption for CO_2 compression.

These conclusions contribute to the development of more-efficient and less cost-intensive technologies for CO_2 capture from power plants.

References

Cousins, A., Wardhaugh, L.T., Feron, P.H.M., 2011. A survey of process flow sheet modifications for energy efficient CO_2 capture from flue gases using chemical absorption. Int. J. Greenh. Gas Control 5, 605–619.

De Miguel Mercader, F., Magneschi, G., Sanchez Fernandez, E., Stienstra, G.J., Goetheer, E.L.V., 2012. Integration between a demo size post-combustion CO_2 capture and full size power plant. An integral approach on energy penalty for different process options. Int. J. Greenh. Gas Control 11S, S102–S113.

EBTF (European Benchmark Task Force), 2011. European best practice guide for assessment of CO_2 capture technologies www.gecos.polimi.it/research/Large_scale_energy.php.

EnergyMarketPrice, 2013. CO_2 emissions at their highest level ever in 2012 www.energymarketprice.com.

Frailie, P.T., Madan, T., Sherman, B.J., Rochelle, G.T., 2013. Energy performance of advanced stripper configurations. GHGT-11 Conference, Kyoto, Japan, November 2012. Energy Procedia 37, 1696–1705.

Freeman, S.A., Dugas, R., Van Wagener, D.H., Nhuyen, T., Rochelle, G.T., 2010a. Carbon dioxide capture with concentrated, aqueous piperazine. Int. J. Greenh. Gas Control 4, 119–124.

Freeman, S.A., Davis, J., Rochelle, G.T., 2010b. Degradation of aqueous piperazine in carbon dioxide capture. Int. J. Greenh. Gas Control 4, 756–761.

Gecos, 2013. GS software www.gecos.polimi.it/software/gs.php.

Giuffrida, A., Bonalumi, D., Lozza, G., 2013. Amine-based post-combustion CO_2 capture in air-blown IGCC systems with cold and hot gas clean-up. Appl. Energy 110, 44–54.

Gunasekaran, P., Veawab, A., Aroonwilas, A., 2013. Corrosivity of single and blended amines in CO_2 capture process. GHGT-11 Conference, Kyoto, Japan, November 2012. Energy Procedia 37, 2094–2099.

IEA Greenhouse Gas R&D Programme, 2012. Operating flexibility of power plants with CCS, IEA report 2012/6.

Jordal, K., Marchioro Ystad, P.A., Anantharaman, R., Chikukwa, A., Bolland, O., 2012. Design-point and part-load considerations for natural gas combined cycle plants with post combustion capture. Int. J. Greenh. Gas Control 11, 271–282.

Knudsen, J.N., Andersen, J., Jensen, J.N., Biede, O., 2011. Evaluation of process upgrades and novel solvents for the post combustion CO_2 capture process in pilot-scale. GHGT-10 Conference, Amsterdam, The Netherlands, September 2010. Energy Procedia 4, 1558–1565.

Leyzerovich, A.S., 2007. Steam turbines: how big can they get? Mod. Power Syst. May 2007, 50–55.

Lin, Y.-J., Madan, T., Rochelle, G.T., 2013. Advanced stripper configurations using piperazine and monoethanolamine. In: 2nd Post Combustion Capture Conference (PCCC2), Bergen, Norway.

Lozza, G., 1990. Bottoming steam cycles for combined gas–steam power plants: a theoretical estimation of steam turbine performance and cycle analysis. In: Proceedings of the 1990 ASME Cogen-Turbo, 83–92, New Orleans (LO), USA.

NETL, 2002. Evaluation of Fossil Fuel Power Plants with CO_2 removal. National Energy Technology Laboratory, Pittsburgh, PA, www.netl.doe.gov/technologies/carbon_seq/refshelf/analysis/pubs/Evaluation_of_Fossil_Fuel_Power_Plants_with_CO_2_Recovery.pdf

NETL, 2003. Greenhouse Gas Emission Control by Oxygen Firing in Circulating Fluidized Bed Boilers: Phase 1 – A Preliminary Systems Evaluation. National Energy Technology Laboratory, Pittsburgh, PA, www.osti.gov/bridge/servlets/purl/825796/825796.pdf

NETL, 2012. Impact of Load Following on Power Plant Cost and Performance: Literature Review and Industry Interviews. www.netl.doe.gov/energy-analyses/pubs/410_01_32_FR_Rev1_20121010.pdf.

Oyenekan, B.A., Rochelle, G.T., 2006. Alternative stripper configurations to minimize energy for CO_2 capture. In: Proceedings of the 8th International Conference on Greenhouse Gas Control Technologies (GHGT-8), Trondheim, Norway.

Pfaff, I., Oexmann, J., Kather, A., 2010. Optimised integration of post-combustion CO_2 capture process in greenfield power plants. Energy 35, 4030–4041.

Rochelle, G.T., Oyenekan, B.A., 2008. Regeneration of an aqueous solution from an acid gas absorption process by matrix stripping, Patent No. US 2008/0127831.

Rochelle, G.T., Chen, E., Freeman, S., Van Wagener, D., Xu, Q., Voice, A., 2011. Aqueous piperazine as the new standard for CO_2 capture technology. Chem. Eng. J. 171, 725–733.

Roeder, V., Hasenbein, C., Kather, A., 2013. Evaluation and comparison of the part load behaviour of the CO_2 capture technologies oxyfuel and post-combustion. Energy Procedia 37, 2420–2431, GHGT-11 Conference, Kyoto, Japan, November 2012.

Singh, P., Van Swaaij, W.P.M., Brilman, D.W.F., 2013. Energy efficient solvents for CO_2 absorption from flue gas: vapor liquid equilibrium and pilot plant study. Energy Procedia 37, 2021–2046, GHGT-11 Conference, Kyoto, Japan, November 2012.

United Nations Framework Convention on Climate Change, 2010. Cancun Climate Change Conference, http://unfccc.int/meetings/cancun_nov_2010/meeting/6266.php.

Van der Ham, L.V., De Kler, R., Matic, A., Goetheer, E.L.V., 2013. Integration of a high-pressure piperazine capture plant with a power plant – an exploratory energetic evaluation. In: TCCS-7 Conference, Trondheim, June 2013.

Van Wagener, D.H., Rochelle, G.T., 2011. Stripper configurations for CO_2 capture by aqueous monoethanolamine and piperazine. GHGT-10 Conference, Amsterdam. Energy Procedia 4, 1323–1330.

Voice, A., Rochelle, G.T., 2011. Oxidation of amines at absorber conditions for CO_2 capture from flue gas. GHGT-10 Conference, Amsterdam. Energy Procedia 4, 171–178.